The Relationship Between Partial Discharge Current Pulse Waveforms and Physical Mechanisms

Key Words: Partial discharge current pulse waveforms, discharge mechanisms, SF_6, gas mixtures, rise time, fall time

H. Okubo, N. Hayakawa, A. Matsushita
Department of Electrical Engineering, Nagoya University, Nagoya, Japan

Partial discharge (PD) measurements have long been recognized as an important tool for detecting and predicting dielectric breakdown (BD) [1], [2]. However, as a result of their small amplitude and wide bandwidth, the relationship between the physical mechanisms of gas breakdown and PD signal generation has not been clarified fully. We have investigated the relationship between PD current pulse waveforms and physical mechanisms to provide a basis for improved PD-based diagnostics.

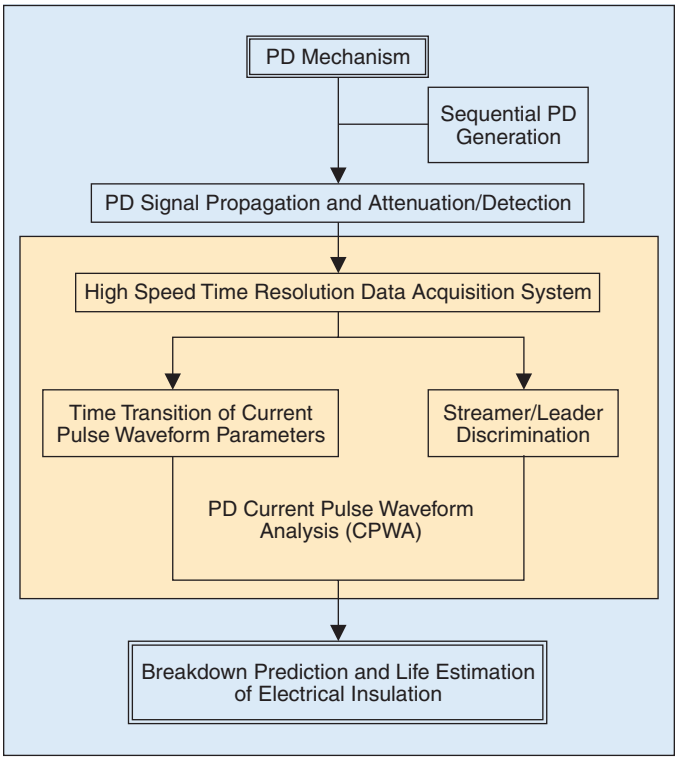

Fig. 1. PD-current pulse waveform analysis (PD-CPWA).

The detailed nature of the PD waveform depends on the PD generating conditions, including gas species, gas pressure, charging, void conditions, etc.

PD waveforms in most apparatus are determined by LC resonances within the apparatus. In transmission line systems such as cables, PD propagation can be free of such resonances but is typically subject to substantial high-frequency attenuation caused by high-frequency losses in the cable dielectric and semiconducting layers. Only in very low loss transmission line systems, such as GIS and GIL, can PD pulses propagate with moderately good fidelity. Even in these systems, high-frequency propagation is limited by the transfer of energy from TEM00 to higher-order modes at discontinuities such as spacers, elbows, etc. Such higher-order modes within the bandwidth of the PD pulse result from the large diameter of such transmission lines. Of course the available PD signal bandwidth for ultra wide band (UWB) PD detection is determined by the nature of the PD pulse. PD pulse rise times can vary from less than 0.35 ns to tens of ns depending on the nature of the PD source. This implies that the PD signal bandwidth can vary from 1 GHz to tens of MHz. The available bandwidth in the PD signal is of great interest both as a diagnostic and as an input to the design of

 0883-7554/02/$17.00©2002IEEE

UWB PD detection systems. Thus an understanding of the physical mechanisms that underlie PD signal generation and determine the PD signal bandwidth is of significant practical importance.

PD current pulse waveforms contain essentially all the available data concerning the PD generation and thus the available information concerning the cause of the PD. The detailed nature of the PD waveform depends on the PD generating conditions, including gas species, gas pressure, charging, void conditions, etc. In addition, the rise time and the fall time of PD current pulse are influenced directly by electron avalanche and/or streamer/leader discharge extension, and by diffusion and recombination of charge carriers, respectively. Analysis of the PD waveform characteristics contributes to the physical understanding of electrical insulation degradation. Figure 1 shows the concept of PD current pulse waveform analysis (PD-CPWA).

In this article, we first describe the technique for measuring PD current pulse waveforms, then the measurement results including the PD current pulse waveform analysis, and finally we apply the results of the PD-CPWA method including BD prediction using streamer/leader discharge discrimination.

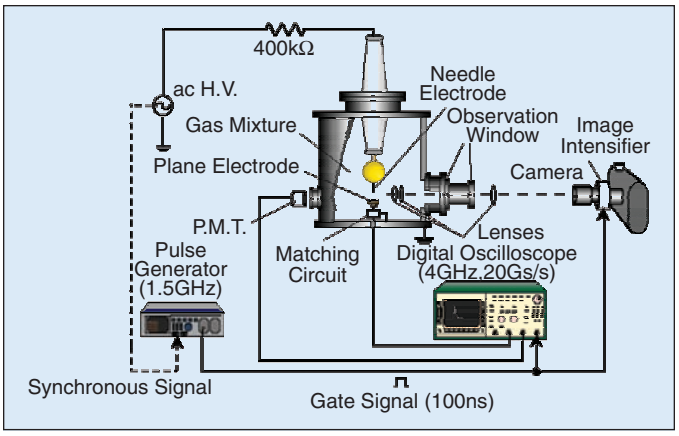

Fig. 2. Experimental setup for waveform measurement.

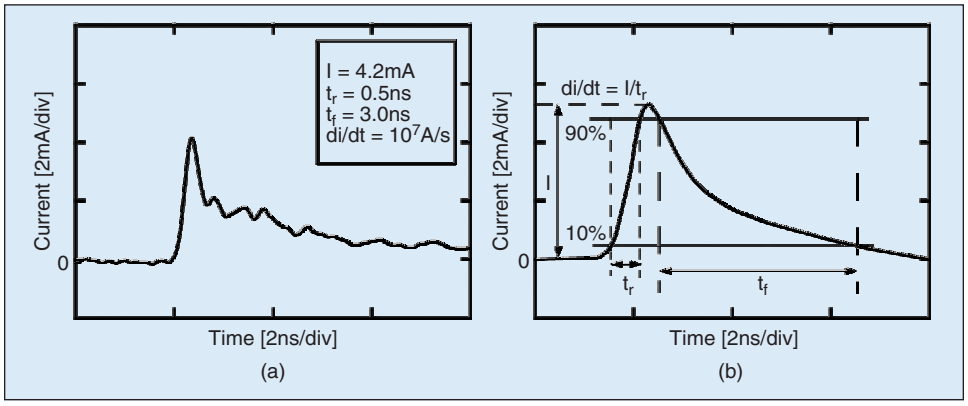

Fig. 3. (a) Definition of PD parameters and (b) current pulse waveform in pure SF_6 gas at 0.1 MPa.

Experimental

Figure 2 shows an experimental setup for the measurement of PD characteristics at power frequency. In order to simulate PD in gas dielectrics, a needle electrode with a tip radius of 0.5 mm and a length of 20 mm was fixed onto the sphere electrode. A plane electrode with a diameter of 30 mm was placed under the needle electrode. The gap length of the needle-plane electrode system was either 10 mm or 20 mm. The test vessel could be filled with different gases or gas mixtures as shown in Table I at pressures of 0.1~0.4 MPa. All experiments reported in this paper were carried out at room temperature.

For the application of PD-CPWA method, it is important to measure the PD current pulses with high accuracy. The PD current pulse waveform was measured by a digital oscilloscope (20 GS/s, 4 GHz bandwidth) through the plane electrode and a matching circuit. The match-

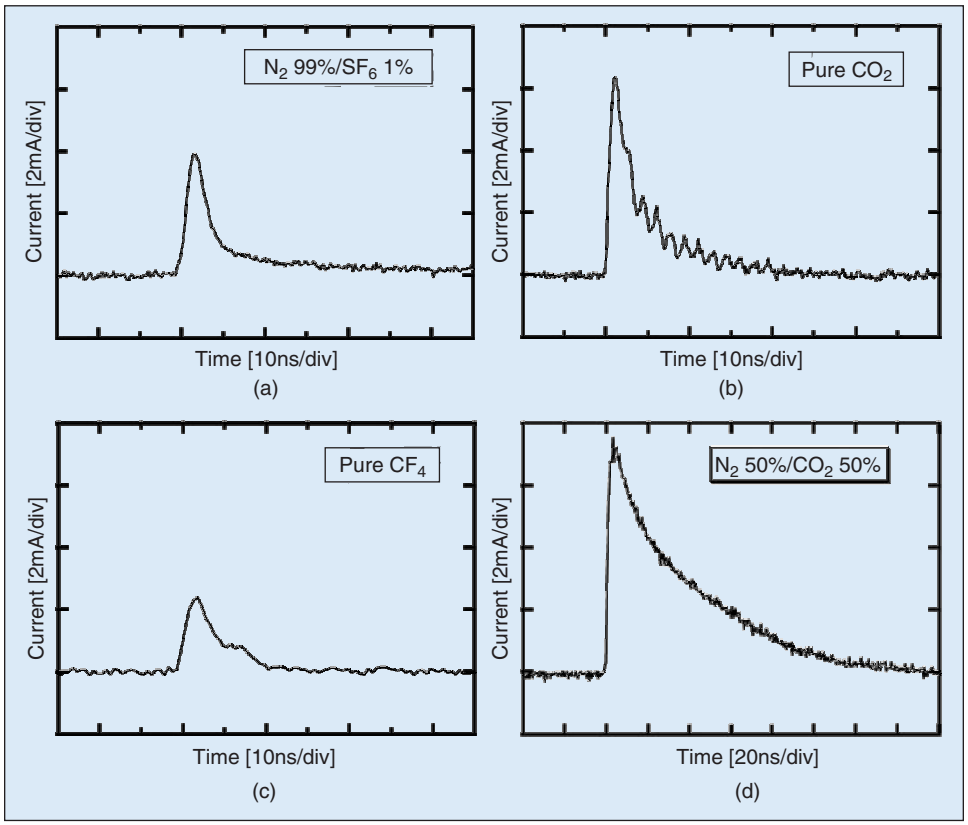

Fig. 4. Positive voltage PD current pulse waveforms at 0.1 Mpa: (a) N_2 99%/SF_6 1%, (b) pure CO_2, (c) pure CF_4, (d) N_2 50%/CO_2 50%.

Table I. Gas Species and Mixture Ratio.		
No.	**Gas Species**	**Mixture Ratio**
1	N_2	100%
2	N_2 / CO_2	50% / 50%
3	CO_2	100%
4	N_2 / CO_2	50% / 50%
5	CF_4	100%
6	SF_6 / N_2	1% / 99%
7	SF_6 / CO_2	1% / 99%
8	C_2F_6	100%
9	C_3F_8	100%
10	SF_6 / N_2	60% / 40%
11	SF_6	100%

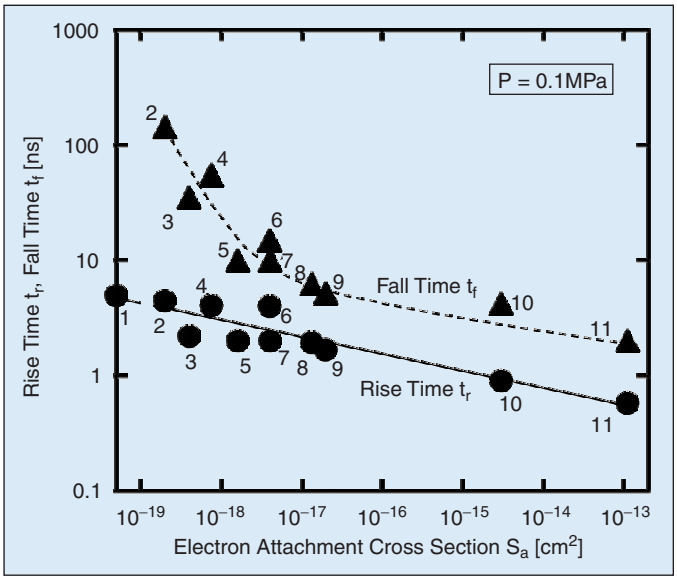

Fig. 5. Rise time, t_r; fall time, t_f, of PD current pulse waveforms as a function of electron attachment cross section (P = 0.1 MPa). The numbers identify the gas or gas mixture in Table II:

Table II. Identification of Numbers in Figure 5.							
No.	N_2	O_2	SF_6	CO_2	CF_4	C_2F_6	C_3F_8
1	1						
2	0.5			0.5			
3				1			
4	0.5	0.5					
5					1		
6	0.99		0.01				
7			0.01	0.99			
8						1	
9							1
10	0.4		0.6				
11			1				

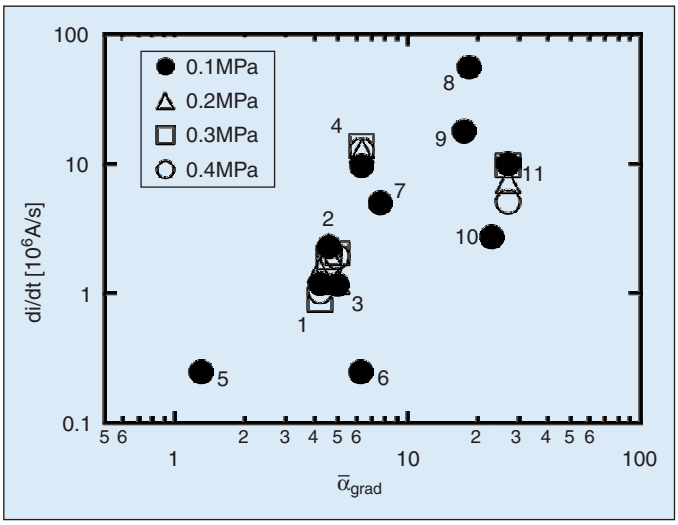

Fig. 6. di/dt as a function of $\bar{\alpha}_{grd}$. The numbers identify the gas or gas mixture listed in Table II.

ing circuit had a high frequency response from dc to over 1 GHz. A single shot PD light emission image was observed using an image intensifier controlled by a pulse generator. The phase-gate control method [3] enabled us to simultaneously measure a single shot PD current pulse waveform, the PD light intensity, and the PD light emission image at the designated phase angle of the applied ac voltage.

PD Current Pulse Waveforms

Definition of PD Current Pulse Waveform Parameters

The positive PD current pulse waveform in pure SF_6 gas is shown in Fig. 3 with the definition of the PD parameters as rise time, t_r; fall time, t_f; and di/dt (= I/t_r, I: PD current pulse height). t_r and t_f in pure SF_6 gas in Fig. 3 are 0.5 ns and 3.0 ns, respectively, and di/dt is 10^7 A/s. The rise time, t_r corresponds to the period of electron avalanche and streamer propagation in the process of PD extension, while t_f corresponds to the period of space charge drift after the PD extension, and di/dt would have a close relationship with the velocity PD extension. Thus, the PD current pulse waveforms contain substantial information about PD physics, such as PD inception and extension mechanisms, etc. These waveform parameters would be changed by gas species and gas pressure.

In the following section, the importance of current pulse waveforms analysis will be clarified by using different gas species and gas mixtures.

PD Parameters Related to Current Pulse Waveforms

Figure 4 shows PD current pulse waveforms for several gases and gas mixtures shown in Table I. The rise time, t_r, corresponds to the electron avalanche process during PD extension, while t_f corresponds to the period of electron drift in the gap space after the PD extension. These processes are related to physical properties of gas species, such as the electron attachment activity in electronegative gases. Figure 5

shows t_r and t_f of streamer discharge in different electronegative gases at 0.1 MPa as a function of the maximum value S_a of the electron attachment cross section. S_a is the maximum value of the electron attachment cross section for a particular gas. For a gas mixture, the value of S_a is the simple arithmetical mean of the two mixed gases. The decrease in t_r with S_a is attributed to the suppression of the electron avalanche due to the increase in electronegativity. The suppression of the electron avalanche also brings about a reduction in the number of electrons in the gap space, resulting in a decrease in t_f. An increase in electronegativity also contributes to the disappearance of electrons in the gap, and results in a decrease in fall time, t_f.

Next, we discuss di/dt in the PD current pulse waveforms. We investigated the relationship between di/dt and $\overline{\alpha}_{grd}$ in component gases. $\overline{\alpha}_{grd}$ is defined by the equation

$$\overline{\alpha}_{grd} = \left(\frac{\alpha - \eta}{P}\right)\left(\frac{E}{P}\right)^{-1} \quad \text{at } E = E_{cr}$$

where $\overline{\alpha}_{grd}$ is the gradient of the effective ionization coefficient [4]-[7] against the electric field strength E at $E = E_{cr}$, where E_{cr} is the critical electric field strength. In other words, $\overline{\alpha}_{grd}$ is the electric field sensitivity of the ionization activity. Gases with higher $\overline{\alpha}_{grd}$ are more sensitive to the electric field distribution. Figure 6 shows di/dt as a function of $\overline{\alpha}_{grd}$ for different gas and gas pressures listed in Table II. di/dt is found to have a positive correlation with $\overline{\alpha}_{grd}$, irrespective of the gas pressure. This result suggests that di/dt depends on the rate of generation of effective electrons at the critical field, irrespective of the electronegativity of the gases.

PD Extension Characteristics

Figure 7 shows El/E_{cr} (El is the electric field strength at the PD tip) as a function of S_a for different gases and gas mixtures at P = 0.1 MPa and as identified in Table II. El/E_{cr} is smaller than 1.0 in most gases and gas mixtures with $S_a < 10^{-17}$ cm^2, which means that PD develops into regions with a lower electric field than E_{cr}. These results suggest that the electron avalanche and streamer propagation in weakly electronegative gases and gas mixtures would be more active compared to the case in strongly electronegative gas like SF_6, and bring about the long PD development. El/E_{cr} is equal to 1.0 in highly electronegative gases such as SF_6 gas, which confirms that PD propagation is limited to the region where the electric field is equal to or higher than E_{cr}. This means that at a pressure of 0.1 MPa, these PD were all streamer type discharge. On the other hand, the PD current pulse waveform also depends on the gas pressure and the applied voltage. Figure 8 shows the gas pressure dependence of the rise time t_r of the PD current pulse and PD light intensity waveforms in SF_6 gas [8]. The rise time, t_r, lies in the subnanosecond time region and increases at gas pressure around 0.3 MPa, which is derived from the transition to a

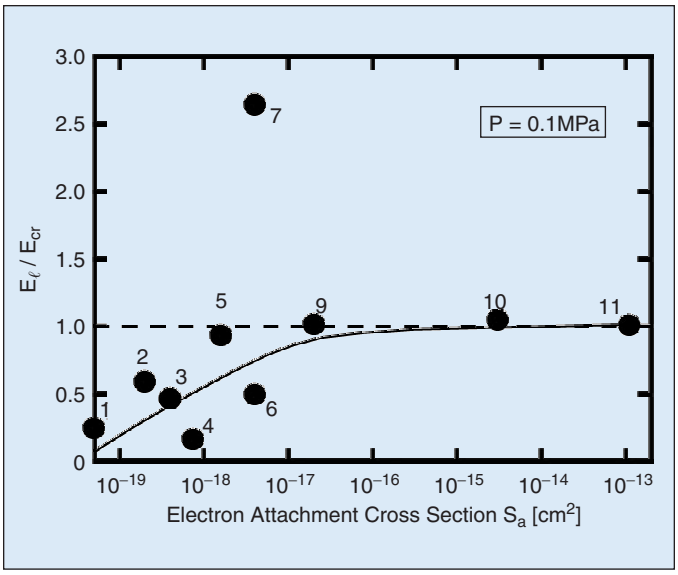

Fig. 7. PD extension characteristics as a function of electron attachment cross section. The numbers identify the gas or gas mixture listed in Table II.

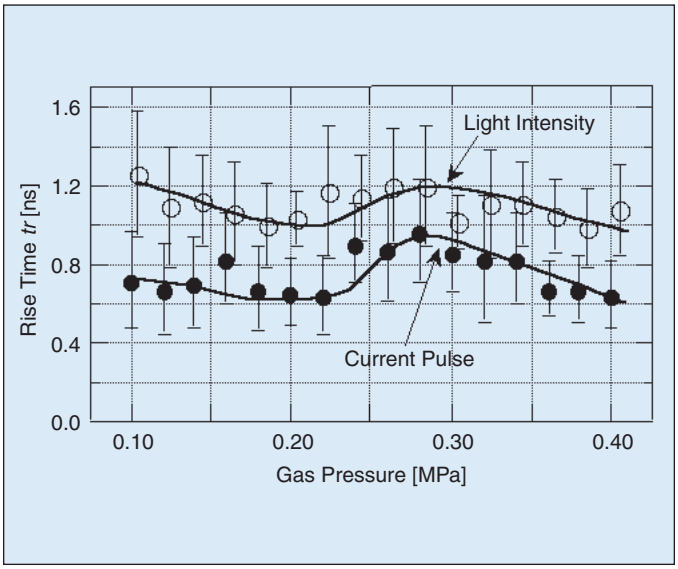

Fig. 8. Gas pressure dependence of current pulse rise time in SF_6.

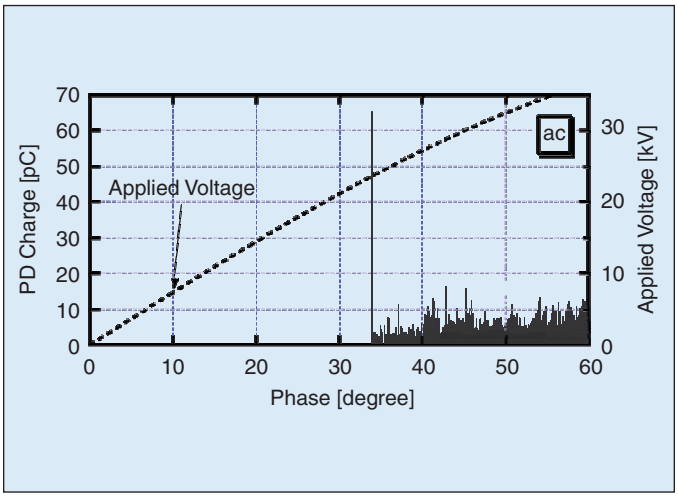

Fig. 9. PD versus phase characteristics.

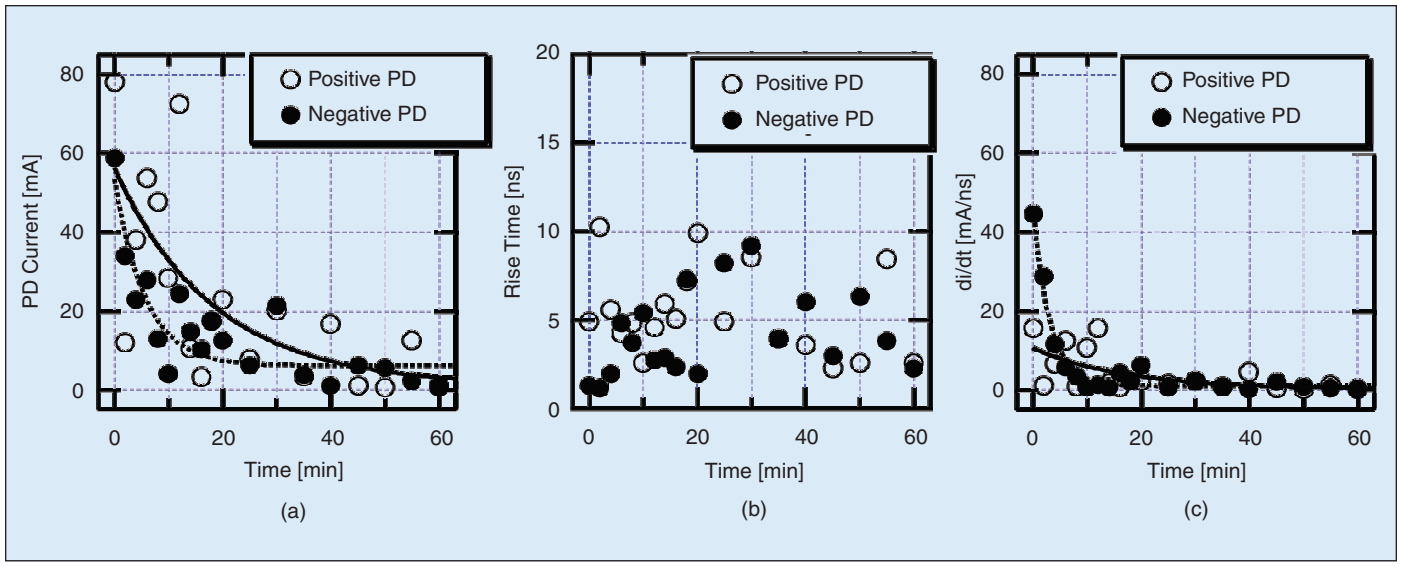

Fig. 10. Variation of PD characteristics with time under voltage, (a) PD current, (b) rise time, (c) di/dt.

leader type discharge with a longer extension length leading to breakdown.

Sequential Generation of PD Pulses

Sequential generation characteristics of the PD as a function of the time during a power frequency waveform are also very important to analyze the PD characteristics and breakdown prediction. Thus the relationship between the space charge behavior and the sequential PD generation should be clarified. Figure 9 shows the typical time-resolved PD characteristics under ac voltage for a needle/plane electrode system in SF_6 gas at 0.1 MPa [9]. The first PD pulse in a positive half cycle has a relatively large charge magnitude, and is followed by subsequent PD pulses with small charge magnitudes. Positive and negative ions generated by PD in the previous negative half cycle could reach the needle and plane electrodes, respectively, and most ions would be neutralized at each electrode surface at the polarity reversal of the applied power frequency voltage. This was verified by ion drift simulation. The residual ions in the gap space would contribute to the generation of positive PD in the subsequent positive half cycle. Thus, the charge magnitude of the first PD is large due to less effective corona stabilization effect of the low residual ion density. Once the first PD is generated, however, the ion density around the needle electrode would create a rich and active corona stabilization effect, resulting in the small charge magnitudes of subsequent PD pulses.

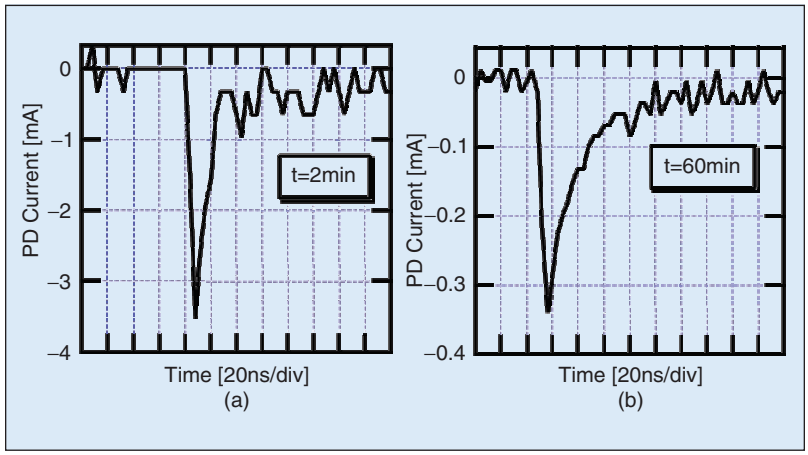

Fig. 11. PD current pulse waveforms, (a) initial stage, (b) final stage.

Variation of PD Pulse Waveform Parameters with Time

High-Speed Time Resolution Data Acquisition System

Based on the above-mentioned characteristics of the PD current pulse waveform, we propose a new technique of PD measurement for understanding the degradation of electrical insulation. In this technique, we needed to establish a high-speed time resolution data acquisition system. In this system, current pulse waveforms of all the PD from the instant of voltage application to BD were precisely measured with subnanosecond time resolution. We introduce here a novel approach based on PD current pulse waveform analysis (PD-CPWA) as shown in Fig. 1 in order to investigate the physical mechanisms of insulation degradation of solid insulators. The CPWA technique focuses on the time transition of individual PD waveform parameters like rise time, fall time, *di*/*dt*, and its frequency spectrum, in the time-resolved waveform of a single PD current pulse.

Example for Creepage Discharge in SF_6

First, we applied the CPWA technique to a rod-epoxy-plane electrode system in SF_6 gas. Figure 10 shows the time variation of (a) PD current pulse height, (b) rise time, and (c) *di*/*dt* in PD current pulse waveforms. Figure 11 shows a single shot of PD current pulse waveforms at (a) the initial stage, and (b) the final stage. In the CPWA technique, not only the long-time PD generation

characteristics, but also the individual single shot PD current pulse waveforms are analyzed. PD current pulse height and *di*/*dt* decrease drastically with time, while the rise time is not time dependent. The decrease in PD current pulse height may be attributed to the decrease in *di*/*dt* as the PD extension velocity associated with streamer extension. Thus, the decrease in *di*/*dt* suggests that the PD generation mechanism would be changed by the influence of charge accumulation on the epoxy surface, etc.

Example for Thermally Degraded Epoxy Spacer

Figure 12 shows an experimental model spacer of thermal degradation. The spacer model was made of epoxy resin with an alumina filler. We confirmed that the normal spacer model was PD free up to 154 kVrms. Thermal degradation was caused by heating the model to 180 °C for five hours; the PDIV after thermal ageing was 141 kVrms. Then, we applied 141 kVrms and the spacer model finally broke down after 682 second (11 minutes, 22 seconds) of voltage application. A total of 5366 PD pulses were measured up to BD. Figure 13 shows the time evolution of the PD generation characteristics from voltage application to BD. As shown in Fig. 13a, the numbers of PDs in the initial stage were very small for about the first 10 minutes, and almost all PDs were of negative polarity. On the other hand, close to BD, the number of positive and negative PDs drastically increased, and the PD current also increased. Figure 13b shows the PD characteristics for the final 60 seconds before BD. As shown in Fig. 13b, the number and amplitude of the PDs of both polarities increased, with some discrete rest times. Figure 13c shows the PD generation immediately before BD. As shown in Fig. 13c, small PDs were detected among the large PDs, immediately before BD. These small PDs were detected before 15 seconds of BD, and it should be pointed out that the small PDs play a role in extending the BD. Figure 13 d shows the last PD leading to BD. Thus, the CPWA technique can be successfully applied to degradation analysis and life estimation techniques because the current pulse waveforms have enough information about the PD characteristics in solid dielectrics so that analyzing the PD parameters would enable us to estimate the progress of the degradation.

Breakdown Prediction by Streamer-Leader Discrimination

As was previously discussed, at higher pressure SF_6 gas, the leader type discharge may lead to breakdown [8]. The CPWA technique is able to discriminate between a harmful leader and a streamer discharge and thus would be a useful tool to predict gas breakdown under certain conditions, for example, certain test geometries in the laboratory or long gap experimental conditions. In GIS, however, a leader is unlikely to occur without having a breakdown, which would limit the ability of the CPWA technique to predict breakdown. As shown in Figs. 14a and b, the streamer discharge is characterized by a short extension length and a single-peak current pulse waveform, while the leader discharge has a relatively long extension length and a double-peak current pulse waveform [8]. In addition, as was shown in Fig. 8, the longer rise times of both

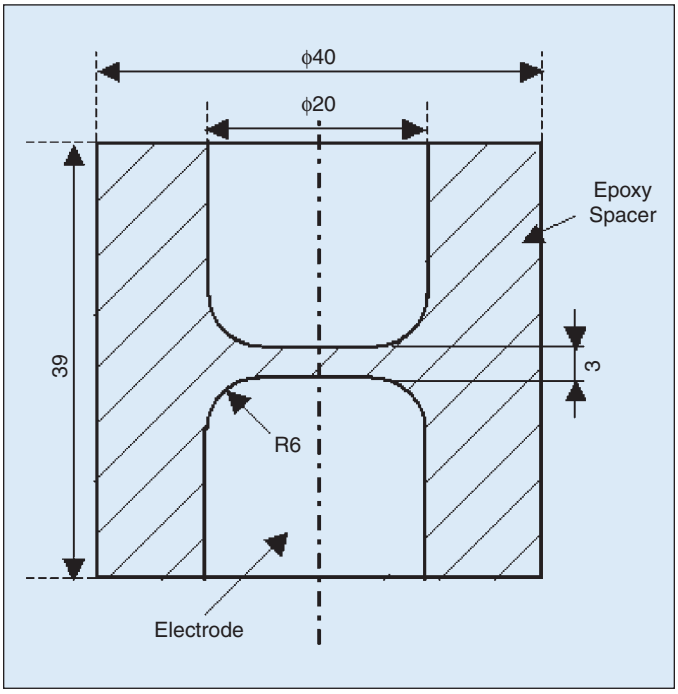

Fig. 12. Spacer model.

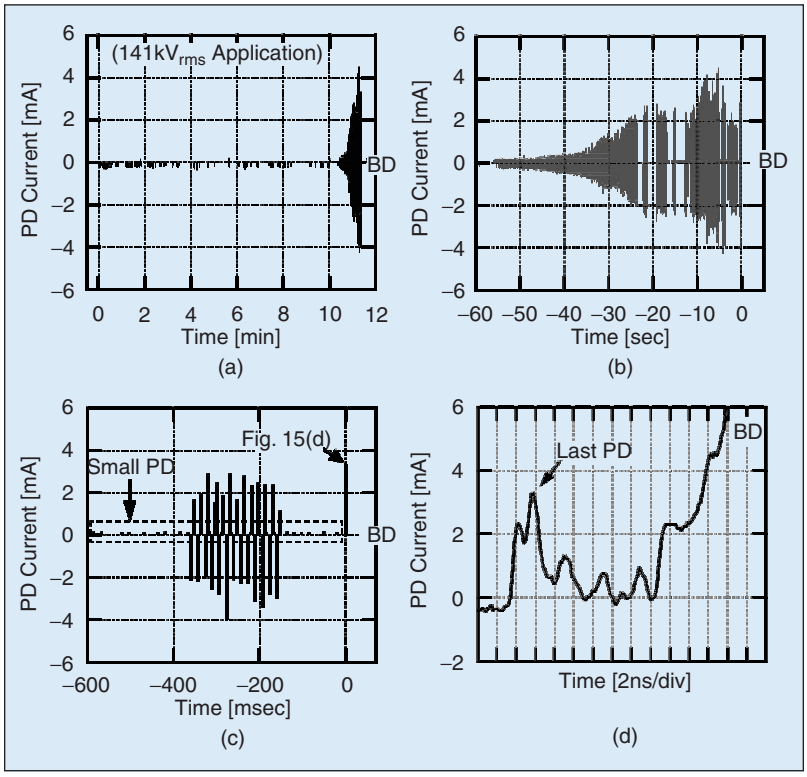

Fig. 13. Variation of PD current with time, (a) total time voltage applied, (b) final minute, (c) final 600 ms, (d) final 30 ns.

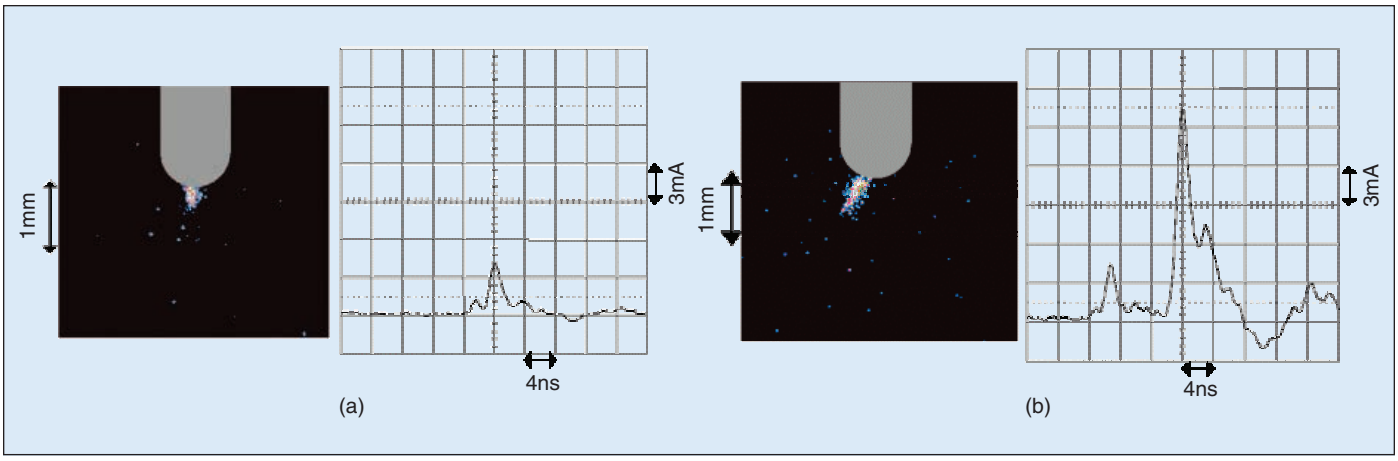

Fig. 14. Discrimination of leader discharge from streamer discharge, (a) streamer [Vertical: 1 div=3 mA; Horizontal: 1 div=4 ns], (b) leader.

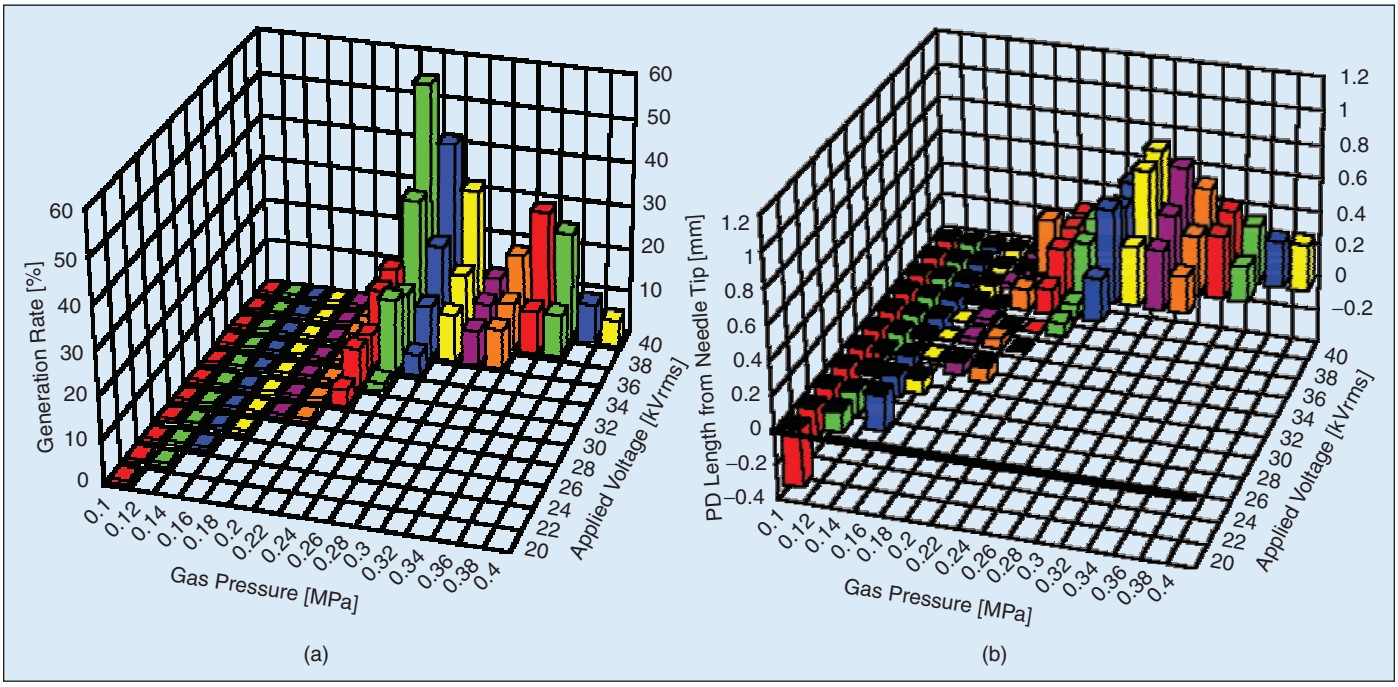

Fig. 15. Leader type discharge generation and double peak pulse generation of PD current pulse, (a) generation rate of double pulses, (b) PD length from needle tip.

the PD current pulse and PD light intensity waveforms at around 0.3 MPa indicate the transition to leader discharge with the long extension length.

Figure 15a shows the generation G_{rate} of double-peak current pulses as functions of gas pressure and applied voltage. Figure 15b, on the other hand, shows the difference between the maximum PD extension length (lm) and critical extension length (ls), where the streamer discharge could extend within the restricted region with an electric field higher than the critical value E_{cr} = 89 V/m/Pa in SF_6 gas. In other words, (lm – ls > 0) means that the PD extends longer than the critical extension length, which corresponds to the leader discharge. The comparison between Figure 15a and b shows the consistency of the pressure-voltage region of the double-peak pulse generation and PD extension longer than ls, resulting in the evidence of leader discharge generation. Thus, the selective PD measurement of double-peak pulse waveform helps to identify a leader discharge and also to predict breakdown in SF_6 gas.

Conclusions

PD current pulse waveforms in gases were measured and analyzed, and the PD mechanisms were clarified. In addition, the PD extension characteristics were discussed from a critical electric field of each gas or gas mixtures viewpoints. The main results in this article are summarized as follows:

1. Rise time t_r and fall time t_f in PD current pulse waveform decreased with increasing the electron attachment cross section S_a in different gases, because of the suppression of electron avalanche in the process of PD extension and the reduction of the number of electrons in the gap space, respectively.

2. A drastic increase in t_f at $S_a < 10^{-17}$ cm^2 may be attributed to the increase in the number of electrons after stopping the PD development together with the longer development of PD.

3. The parameter of *di*/*dt* (pulse height/rise time) in PD current pulse waveforms has a positive correlation with the electric field sensitivity $\overline{\alpha}_{grd}$ of the effective ionization coefficient, irrespective of gas pressure. This suggests that *di*/*dt* will depend on $\overline{\alpha}_{grd}$, with consideration of electronegativity.

4. PD measurement of double-peak pulse waveform enables us to identify the harmful leader discharge leading to breakdown from streamer discharge. This knowledge will contribute to the breakdown prediction technique in the future.

We proposed the PD-CPWA method, which enables us to clarify the relationship between the PD current pulse waveforms and physical mechanisms, and thus may contribute to the development of breakdown prediction and lifetime estimation of electrical insulation of power equipment.

Acknowledgment

The authors wish to express their great appreciation to Dr. Steven Boggs of University of Connecticut, USA, for his valuable and fruitful discussions.

References

1. S. Boggs and J. Densley, "Fundamentals of Partial Discharge in the Context of Field Cable Testing," *Electrical Insulation Magazine*, vol. 16, no. 5, pp.13-18, 2000.
2. H. Okubo, M. Yoshida, T. Takahashi, T. Hoshino, M. Hikita, and M. Miyazaki, "Partial Discharge Measurement in a Long Distance SF_6 Gas Insulated Transmission Line (GIL)," *IEEE Transactions on Power Delivery*, vol. 13, no. 3, pp. 683-690, 1998.
3. T. Takahashi, T. Yamada, N. Hayakawa, and H. Okubo, "Power Frequency Dependence of Space Charge Behavior and Partial Discharge Characteristics in SF_6 Gas," *IEEE Transactions on Dielectrics and Electrical Insulation*, vol. 7, no. 1, pp. 152-160, 2000.
4. L.G. Christophorou and L.A. Pinnaduwage, "Basic Physics of Gaseous Dielectrics," *IEEE Transactions on Electrical Insulation*, vol. 25, no. 1, pp. 55-74, 1990.
5. S.R. Hunter, J.G. Carter, and L.G. Christophorou, "Electron Attachment and Ionization Processes in CF4, C2F6, C3F8, and n-C4F10," *Journal of Chemical Physics*, vol. 86, no. 2, pp. 693-703, 1987.
6. R.D. Hake, Jr. and A.V. Phelps, "Momentum-Transfer and Inelastic-Collision Cross Sections for Electron in O2, CO, and CO2," *Physical Review*, vol. 158, no. 1, pp. 70-84, 1967.
7. M.A. Harrison and R. Geballe, "Simultaneous Measurement of Ionization and Attachment Coefficients," *Physical Review*, vol. 91, no. 1, pp. 1-7, 1953.
8. H. Okubo, T. Takahashi, and N. Hayakawa, "Investigation of Partial Discharge Mechanism and Breakdown Prediction Technique in SF_6 Gas Insulated Systems," *Fourth Workshop & Conference on EHV Technology, Workshop Papers*, pp. 8-14, 1998.
9. T. Takahashi, T. Yamada, N. Hayakawa, and H. Okubo, "Space Charge Behavior in SF_6 Gas and Sequential Generation of PD Pulses," *IEEE Trans. on Dielectrics and Electrical Insulation*, vol. 7, no. 1, pp. 141-145, 2000.

Hitoshi Okubo was awarded a Ph.D. in 1984 in Electrical Engineering from Nagoya University. He joined Toshiba Corporation/Japan in 1973 and was a manager of the high voltage laboratory of Toshiba. From 1976 to 1978, he was at the RWTH Aachen/Germany and the TU Munich/Germany. Since 1989, he was an Associate Professor and presently he is a Professor in the Department of Electrical Engineering at Nagoya University. He is a member of IEEE, IEE of Japan, VDE, and CIGRE.

Naoki Hayakawa received his Ph.D. in 1991 in Electrical Engineering from Nagoya University. Since 1990, he has been a member of the faculty of Nagoya University. Presently, he is an Associate Professor in the Department of Electrical Engineering. He is a member of IEEE and IEE of Japan.

Akihisa Matsushita received the B.S. degree in 2000 in Electrical Engineering from Nagoya University. Presently, he is studying for his Masters degree at the Department of Electrical Engineering, Nagoya University.